

## Raman, PL & AFM measurements on laser lithographically written structures in Si

Silicon (Si), being the second most common element in the earth's crust, is the material most widely used for integrated circuits as well as solar cells. Modern integrated circuit devices work with structures down to 14nm in size[1] and whilst the latest developments use a variety of different technologies, traditionally the structures in semiconductor devices are produced using lithography. In order to ensure the highest quality in the devices, the production steps need to minimize stress and stress induced artifacts in the devices. Other structures in which layers with different lattice constants are grown on top of each other need the strain for lattice matching. It has been shown [2,3] that Raman measurements can effectively probe the strain state of crystalline materials and thus provide an effective, non-destructive way of developing the most appropriate production processes. From solar cell research it is additionally known that stress and crystallinity in Si has a strong effect on the photoluminescence (PL) signal of the Si [4].

In this application note we report on structures in crystalline Si written by laser lithography which were in turn examined on the same instrument using Confocal Raman Imaging, Confocal PL Imaging and AFM.

### Experimental

The experiments were performed using an alpha300 RA Confocal Raman-AFM. The XY positioning of the sample for scanning and lithography was achieved using a piezoelectric scanning stage. A stepper motor was used for the focus control (10nm single step). With this system all experiments could be performed as follows:

#### a) Lithography

The system was equipped with a pulsed 532nm laser (typically employed for fluorescence lifetime imaging microscopy – FLIM) which was used for laser scribing in combination with the DaVinci Lithography package. The CW laser power of the laser was 15mW with a repetition rate of 20MHz and a pulse duration of 20ms. The scripting function of the lithography package allowed not only the arbitrary movement of the sample in XY but also the upward movement of the microscope (to defocus the laser beam) when a movement without laser scribing is desired. Alternatively, an electronic shutter could have been used to achieve this.

#### b) Confocal Raman Imaging

An additional frequency doubled Nd:YAG laser emitting 532nm (CW - continuous wave) was used for confocal Raman imaging which delivered 20mW optical power. The 100X NA 0.9 objective used allowed the laser to focus to a diffraction-limited spot with a diameter of 355nm. The signal was collected using a 25µm core diameter optical multimode fiber which acted as a pinhole to achieve the best depth resolution. A UHTS 300 spectrometer in combination with a 1800g/mm grating and a back-illuminated CCD camera was used for

detection. The integration time per spectrum was 12.2ms. Two scans were performed on the laser scribed area: A planar scan in the XY area (50x50µm<sup>2</sup> with 200x200 points) and a depth scan in the XZ plane (20x5µm<sup>2</sup> with 200x50 points).

#### c) Confocal PL Imaging

For confocal PL imaging the same laser as for Raman imaging was used. In this case a specially selected 50X NA 0.8 objective was chosen which allowed the best throughput for the PL signal (in the range of 1000 - 1250nm for Si) while showing minimal chromatic aberration between the excitation wavelength (532nm) and the PL peak. A 100µm core diameter multimode fiber was used to collect the signal and deliver it to a SpectraPro 2300i mirror based spectrometer using a 150g/mm grating and an InGaAs CCD camera 1024 pixels in width. A scan of 50x50µm<sup>2</sup> with 100x100 points and 0.210s integration time per spectrum was performed.

#### d) Atomic Force Microscopy

The measurements were performed in AC mode using a force modulation cantilever (Nanoworld) with a resonance frequency of 87kHz. The first overview scan was performed on an area of 50x50µm<sup>2</sup> with 512x512 points. A second scan was performed with 14x14µm<sup>2</sup> and 256x256 points.

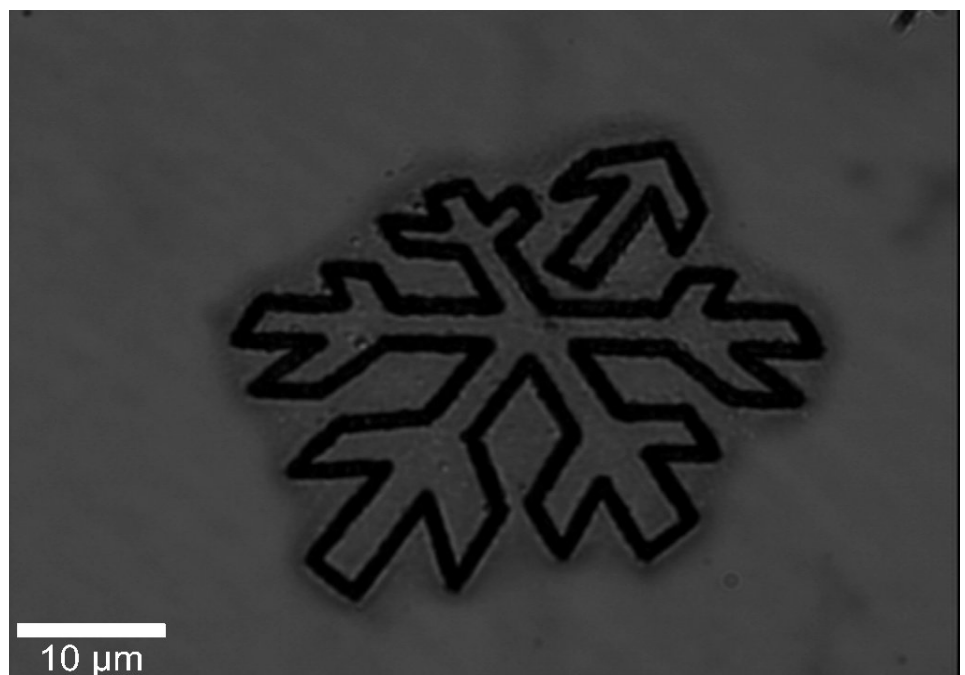


**Fig. 1:** White light image of the lithographically written structure in Si.

## Results

The lithography process for writing the structure took approximately 2 minutes at this laser power. Following this, the white light image as shown in figure 1 could be seen. The image was recorded with the WITec Control software using the built-in video camera.

Following the planar confocal Raman image scan figure 2a could be extracted from the integrated intensity of the first order Si band near 520 rel.1/cm. Figure 2b shows the intensity profile along the blue cross section shown in figure 2a.

The image as well as the cross section show an increased intensity of the Si signal close to the laser scribed structure as well as a strong decrease exactly along it. The cross section reveals a FWHM of the

intensity profile of 680nm. Since the system is diffraction-limited, the laser for scribing the structures was as narrow as 355nm full width half maximum (FWHM) ( $0.6\lambda/NA = 0.6 \times 532\text{nm}/0.9 = 355\text{nm}$ ). When scanning the same structures again with a diffraction-limited resolution the Gaussian profile of the laser during the Raman measurement is convoluted with the geometry of the structure itself. Since the scribing is a thermal process, it is not surprising, that the detected structures are slightly larger than diffraction-limited. The brighter and darker areas in figure 2a suggests that this could be caused by differences in the height of the sample. In such a case the brighter areas could be lying in an optimal focal plane and the dark areas in planes which are not well in focus. In order to check this, a depth scan was performed along the line marked in green in figure 2a. The

result can be seen in figure 3a where the integrated intensity of the 1st order Si peak is shown. It can clearly be seen, that the intensity originates from approximately the same height and that only very little signal is originating from the positions where the laser-scribed structures are. It can additionally be noted that brighter areas are located right next to the structures. This is in agreement with the results as seen in figure 2a where higher intensity is detected right next to the structures. Figure 3b shows the intensity profile extracted along the turquoise line. The sharpness of this profile is partly due to the high depth resolution achievable with the system and partly due to the limited penetration depth of the laser light into Si.

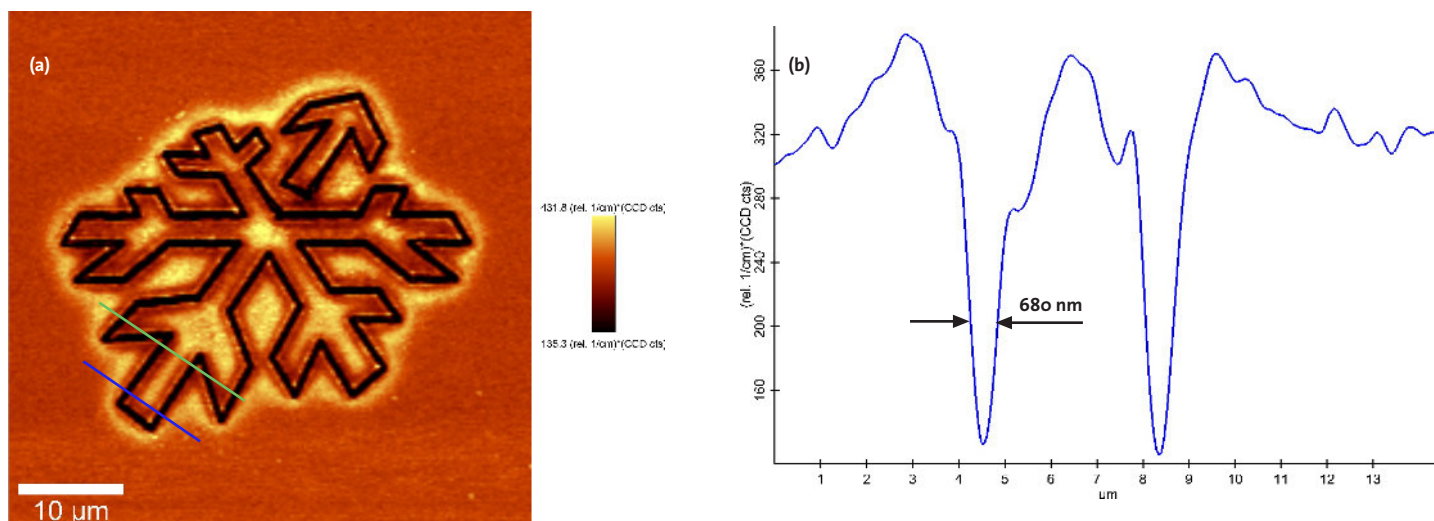


Fig. 2: Confocal Raman Image of the intensity of the first order Si line [a] and the intensity profile along the cross section marked in blue [b]. The green line in [a] indicates where the depth scan was performed.

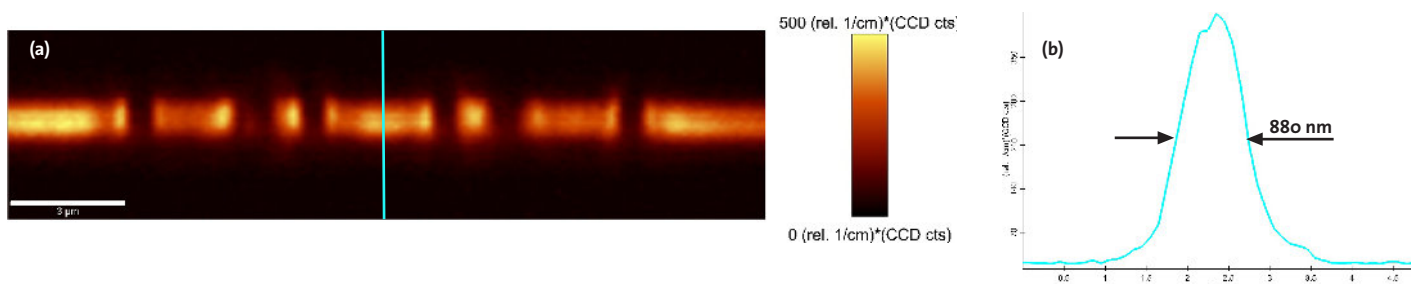


Fig. 3: Confocal Raman Image of the intensity of the first order Si line along a depth scan [a] and the intensity profile along the cross section marked in turquoise [b].

In order to probe the strain state of the Si around this structure, the data acquired in the planar as well as in the depth scan was analyzed in terms of peak shift of the first order Si peak. For the analysis the advanced fitting option in the WITec Project Plus software was used and a Lorentzian curve was fitted to the spectra. From the results the exact position of the peaks could be extracted and this is plotted for the planar scan in figure 4a and for the depth scan in figure 4c. Figure 4b shows two representative, averaged spectra with the corresponding fitted Lorentzian curves. The red curve is representative of the red regions and the blue curve of the blue-purple regions. The peak shift can clearly be seen from this and it is also obvious that the Lorentzian fit follows the data

points extremely well which also demonstrates the imaging quality of the UHTS 300 spectrometer (see also [5]). The shift to lower wavenumbers at the edges of the structures is obvious in both scans. This is indicative of compressive stress in the crystalline structure at these positions.

In order to further examine the laser scribed structures, a confocal PL scan was performed as well. Figure 5a shows the integrated intensity of the Si PL signal and in figure 5b the PL spectrum itself is shown. This spectrum was acquired with 210ms integration time right in the center of the structure and only the camera background signal was subtracted (no smoothing or averaging was applied). The second order peak of the excitation

wavelength at 1064nm can also be seen in this spectrum. Since Si is an indirect semiconductor, the PL efficiency is extremely low compared to i.e. GaAs. Therefore, only a highly effective detection beam path allows the measurement of the PL signal from a diffraction-limited point with integration times similar to those necessary for Raman imaging.

Similar to the previously seen confocal Raman image (figure 2a), the intensity of the signal is stronger close to the structures. The signal was also examined for peak shifts, but did not show a significant change. It has been shown, however, that more elaborate fitting models also allow the extraction of the stress in Si structures from the PL signal [4].

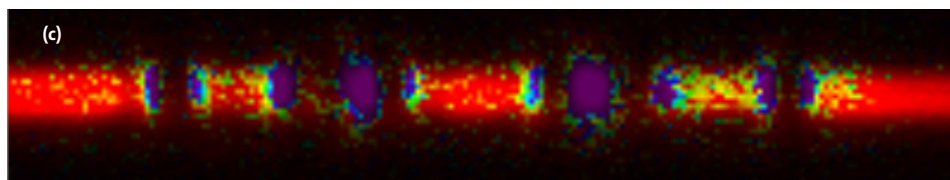
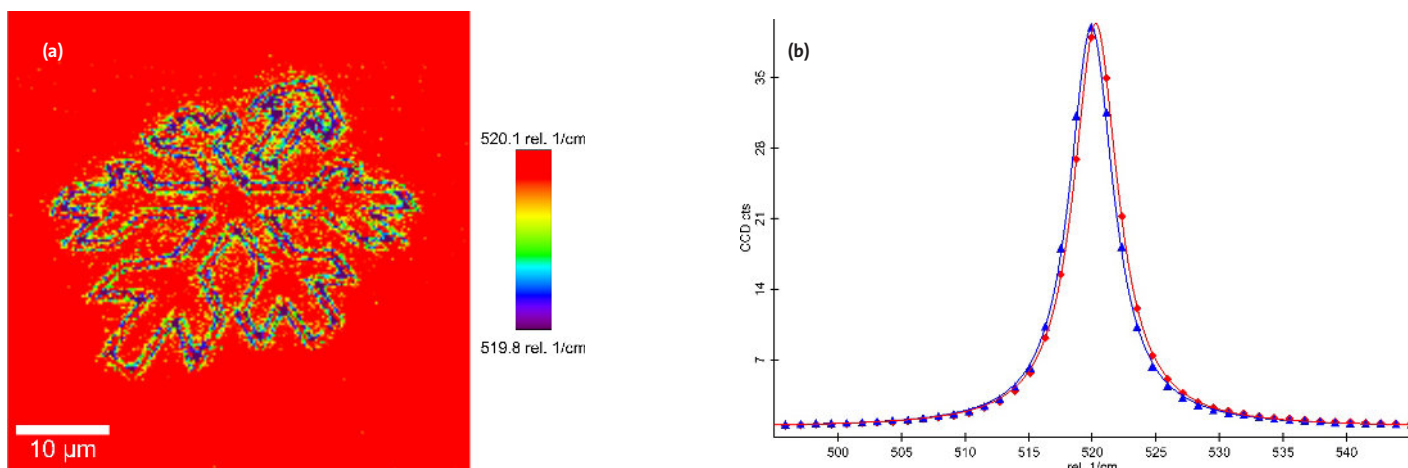


**Fig. 4:** Confocal Raman Image of the position of the first order Si line in the planar scan [a] and in the depth scan [c]. Two representative spectra showing the shift are shown in [b].

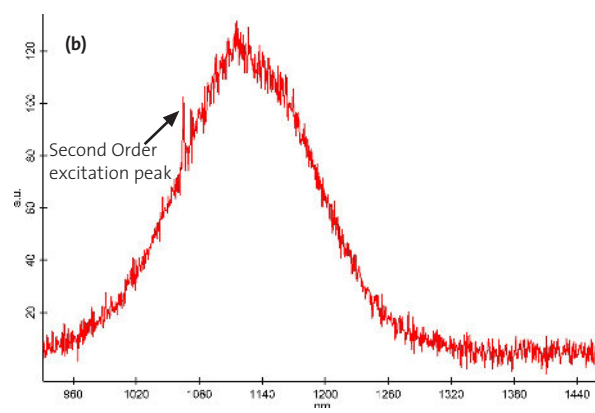
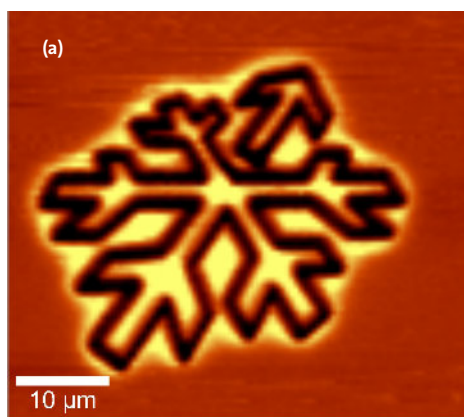


**Fig. 5:** Confocal PL Image of the intensity of the PL signal of Si in a planar scan [a] and a representative PL spectrum which originates from the center of the structure [b].

The PL and the Raman scans clearly showed that where the laser scribing took place, the structures emitted a weaker Raman and PL signal. Looking at the depth scan, however, it seemed puzzling that inside the structures no signal was detected. If the laser scribing had generated grooves then one would have expected the signal at a lower depth if the grooves were not extremely narrow and deep. In order to clarify this question, AFM scans were performed on the structure. Figure 6a shows an AFM overview scan and figure 6b a zoomed in scan focusing on one of the arrows.

Both AFM images clearly show higher topography along the structure and from figure 6b it can clearly be seen that dot-like structures are present along the written structure. At a distance of more than 10µm from the structure, none of these features were visible. The extent of the elevated structures range from about 1 to 2µm FWHM and the dots approximately range in diameter from 300-600nm.

The AFM images indicate that significant structural changes occurred in the Si where the laser scribing

took place. The significantly lowered Si signal near 520 rel.1/cm in combination with the AFM images could indicate that the crystalline structure of the Si was destroyed. In such a case one could expect to see traces of amorphous Si along the structures. In order to check this, the average spectrum far away from the structure and the average spectrum inside the grooves were calculated from the planar Raman data set and are shown in figure 7.

The spectra clearly show the strong decrease in the intensity of the 1st order Si peak, but also an increase in the signal background. It is striking that the background is higher on the low-wavenumber side of the Si peak compared to the high wavenumber side of it. Since amorphous Si shows a broad peak in this region, one could postulate that the material generated through the laser scribing is in some ways related to amorphous Si.

### Conclusion

In a single microscopy system laser scribing, confocal Raman imaging, confocal PL imaging and AFM were performed on a crystalline Si sample. All

experiments were controlled through the same electronics (alphaControl) and the same software (WITecControl). The written structures are clearly detectable with all measurement techniques. The Raman as well as the PL signal originating from crystalline Si is strongly reduced at the laser scribed structures and a broad enhancement of the signal background of the Raman Si signal can be detected. AFM measurements allowed the exclusion of narrow grooves being the origin of the reduced Raman and PL signal and showed that the structures consist of dot-like elevations.

### References

- [1] <http://www.intel.com/content/www/us/en/silicon-innovations/silicon-technologies-general.html>
- [2] Gigler A.M., Huber A.J., Bauer M., Ziegler A., Hillenbrand R. and Stark R.W. (2009), Nanoscale residual stress-field mapping around nanoindentations in SiC by IR s-SNOM and confocal Raman microscopy. *Optics Express*, 17, 22351-22357.
- [3] Wermelinger T., Borgia C., Solenthaler C. and Spolenak R. (2007), 3-D Raman spectroscopy measurements of the symmetry of residual stress fields in plastically deformed sapphire crystals. *Acta Materialia*, 55, 4657-4665.
- [4] Gundel P., Schubert M.C. and Warta W. (2009), Simultaneous stress and defect luminescence study on silicon. *Phys. Status Solidi A*, 207, 436-441.
- [5] Dieing T. and Hollricher O. (2008), High-resolution, high-speed confocal Raman imaging. *Vibrational Spectroscopy* 48; 22-27

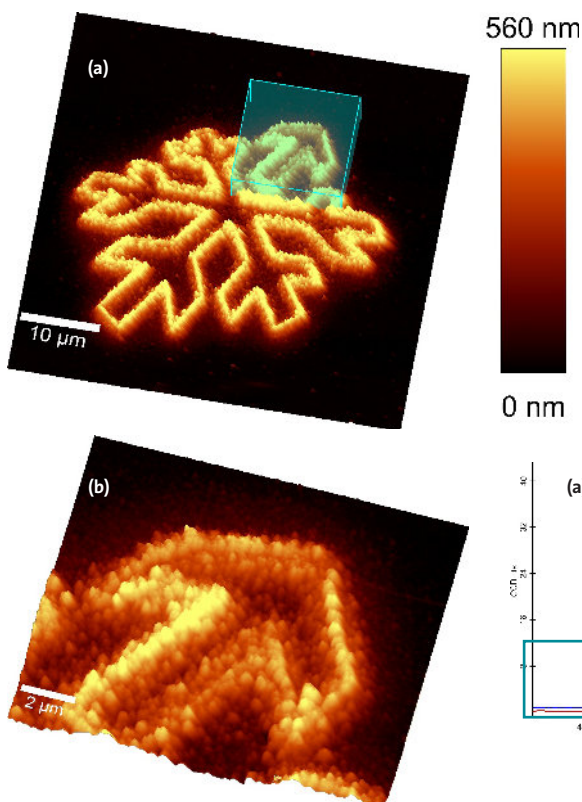


Fig. 6: AFM Scan of the structure. Overview[a] and zoomed scan onto one of the structures[b].

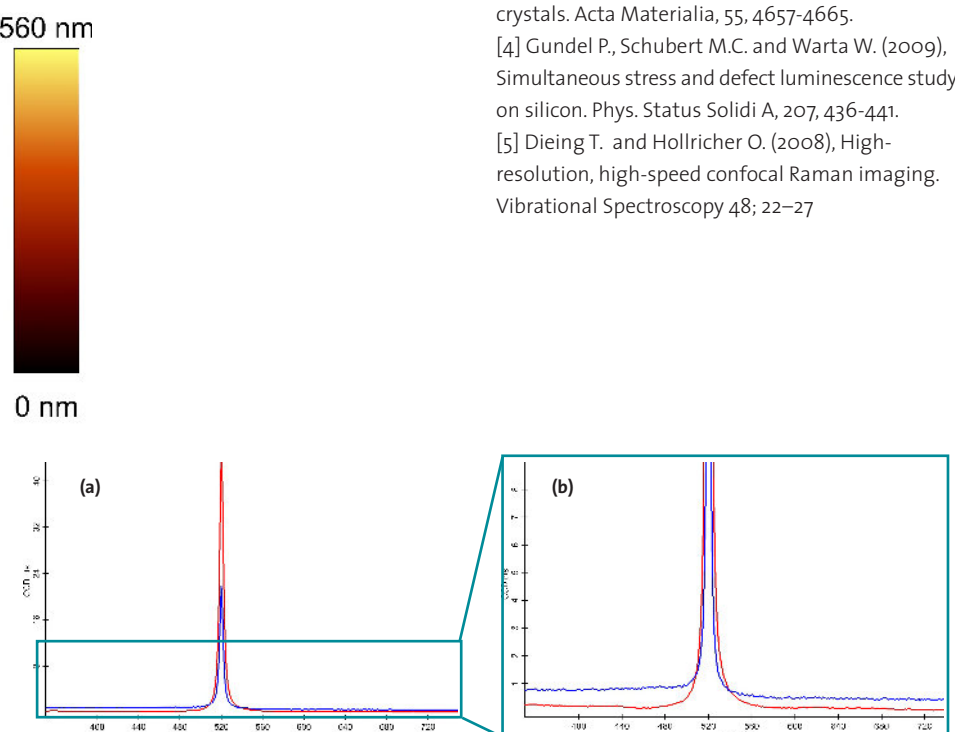


Fig. 7: Raman Spectra well outside the structure (red) and inside the grooves (blue)